Supporting Information

Self-Healing Epoxy Resin Film Enabled by Synergetic Coumarin and MXene

Bingrui Shi, Kaiming Yang, Yifeng Zhang, Feifei Wang, Wenyan Liu, Yekun Zhang, Hongxia Yan*

Supporting information S1

S1.1. Materials

Epoxy resin (E51) was purchased from Guangzhou Suixin Chemical Co., Ltd. Isophorone diisocyanate (IPDI), esculetine (DDCm-OH) and triethylenetetramine (TETA) were obtained from Shanghai Macklin Biochemical Co., Ltd. 1,2-propanediol (PPG) and tetrahydrofuran (THF) was acquired from Shanghai Aladdin Biochemical Technology Co., Ltd. Ti_3C_2 (MXene) was acquired from FoShan XinXi Technology Co., Ltd. Other experimental materials, such as the absolute ethanol and glass instruments, were provided by Xi'an Haotian Chemical Glass Instrument Co., Ltd.

S1.2. Characterizations

The chemical composition of DDCm-EP was determined by fourier transform infrared spectroscopy (FT-IR, Nicolet iS50, U.S.A.). The ^{1}H-NMR and ^{13}C-NMR measurements of DDCm-EP and DDCm-OH were performed on Bruker Avance (500 MHz) spectrometer using DMSO-d_6 as solvent. The molecular weight and distribution of DDCm-EP were determined by gel permeation chromatography (GPC, Waters 2414, U.S.A.) using N,N-dimethylformamide (DMF) as the mobile phase.

The X-ray diffraction (XRD) patterns of MXene, MAX and films were recorded on a Bruker D8 Advance X-ray diffractometer with Cu Kα radiation (λ=0.15405 nm). The 2θ-angular regions between 5° and 70° were investigated with the scanning rate of 0.02°·s^{-1}. The chemical composition of MXene was determined by X-ray photoelectron spectroscopy (XPS, Kratos AXIS Ultra DLD, Britain). The surface morphology of MXene was observed by field emission scanning electron microscopy (SEM, FEI Verios G4, U.S.A.) and high resolution transmission electron microscopy (TEM, FEI Talos F200X, U.S.A.), and the element distribution was obtained.

Thermogravimetric analysis was performed on a synchronous thermal analysis (TGA 8000, U.S.A.) at a heating rate of 10℃·min^{-1} in a nitrogen atmosphere. Dynamic thermo-mechanical analysis (DMA, Hitachi 7100, Japan) was performed in a tensile mode with a frequency of 1 Hz and sample size of 5 mm×5 mm×0.1 mm. The cross-linking density of the samples were measured by low field nuclear magnetic resonance instrument (LF-NMR, Niumag PQ001, China). The samples were put into a solid nuclear magnetic tube with a diameter of 10 mm, the sample height was about 1 cm, and the test temperature was 90℃.

According to GB/T 1040.3-2006 standard, the tensile strength of the sample was studied by electromechanical universal testing machine (CMT 8505) under the condition of tensile speed of 10 mm/min. 5 samples were prepared for each sample, with a size of 50 mm×10 mm×0.1 mm. Tungsten filament scanning electron microscope (SEM, TESCAN VEGA 3 LMH, China) was used to observe the tensile section morphology of the samples under certain magnification and high pressure (20 kV).

The self-healing efficiency is expressed by the tensile strength of the sample before and after repair. The temperature change of the samples under 808 nm laser were tested by the photothermal heating system (CNI MDL-III-808-2W, China). Thermal imaging photographs were performed every 1 min, and the sample test size was 1 cm×1 cm, where the power density of the 808 nm laser was 1.5 W/cm^2.

Supporting information S2

S2.1. Synthesis of DDCm-EP

Initially, a mixture of 4.2 g IPDI, 1.0 g DDCm-OH, 11.9 g PPG and 7.5 g E51 was introduced into a three-necked flask and stirred at 70℃ under a nitrogen atmosphere for 4 hours to create an epoxy prepolymer incorporating coumarin groups (DDCm-E51). Following that, 0.9 g curing agent TETA were combined with DDCm-E51, and the well-blended mixture was then poured into the mold.

Subsequently, the mold underwent curing in a blast drying furnace, with the curing process comprising 12 hours at 25℃ and an additional 2 hours at 60℃. After the curing process, the mold was allowed to naturally cool to room temperature, resulting in the formation of a light-triggered self-healing epoxy resin resin film (DDCm-EP).

It is worth noting that TETA is an amine curing agent. Compared with other curing agent, amine curing agent contain the active -NH-, which allows the epoxy group to open the ring at a lower temperature and does not require a catalyst. This makes the procedure for TETA's cured epoxy prepolymers simple by mixing the two evenly. And TETA requires a low curing temperature, generally can be cured at room temperature. Therefore, we choose the curing method of 12 h/25℃+2 h/60℃. At the same time, the dosage of TETA was calculated according to the ratio of active H to epoxy group as 1:1.

S2.2. FT-IR result of DDCm-EP

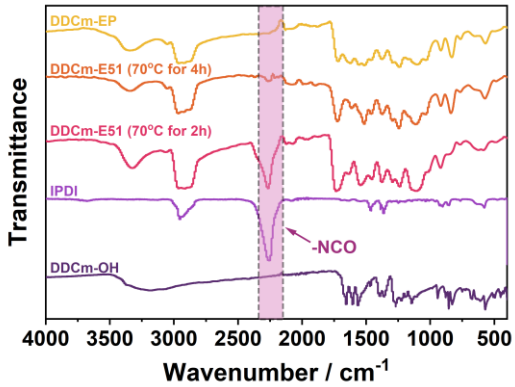

Fig. S1 FT-IR of DDCm-OH, IPDI, the reaction of DDCm-E51, and DDCm-EP

In order to determine whether the reaction proceeded as expected, the raw material DDCm-OH, the raw material IPDI, the reaction of DDCm-E51, and the product DDCm-EP were characterized by infrared spectroscopy, and the results were shown in Fig. S1. To ensure the synthesis of DDCm-E51, FT-IR spectroscopy was performed for DDCm-E51 after reaction at 70℃ for 2 hours and 4 hours, respectively. The results indicated that the intensity of the -NCO peak decreased after 2 hours of reaction at 70℃, suggesting that some -NCO groups had participated in the reaction and been consumed, although a significant amount of -NCO remained, indicating that

the reaction was not yet complete. After 4 hours of reaction at 70°C, the -NCO peak almost completely disappeared, suggesting that the reaction had been completed and DDCm-E51 had been successfully synthesized as expected. Consequently, based on the successful synthesis of DDCm-E51, we proceeded with the subsequent synthesis of DDCm-EP and MXene/DDCm-EP.

S2.3. NMR result of DDCm-EP

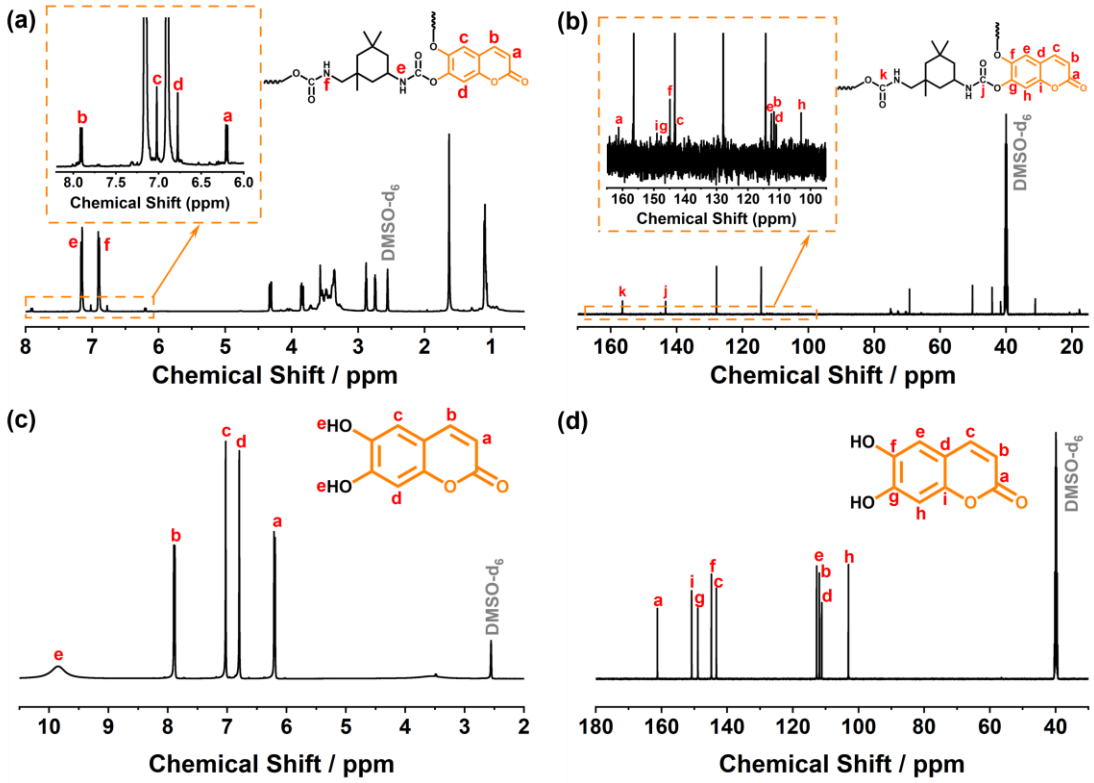

Fig. S2 ^{1}H-NMR (a) and ^{13}C-NMR (b) of DDCm-EP in DMSO-d_6; ^{1}H-NMR (c) and ^{13}C-NMR (d) of DDCm-OH in DMSO-d_6

DDCm-EP was characterized using ^{1}H-NMR and ^{13}C-NMR, as depicted in Figure S2. Figure S2(a) shows the ^{1}H-NMR spectrum of DDCm-EP, with DMSO-d_6 selected as the solvent. The ^{1}H-NMR signal peaks cover the protons of the coumarin group and the N-H proton of the carbamate bond. The coumarin group protons are observed in the range of 6.18-7.92 ppm (a-d), while the carbamate bond N-H protons are observed at 7.17 ppm (e) and 6.89 ppm (f). It is noteworthy that the small amount of DDCm-OH added results in a low intensity of the nuclear magnetic resonance signals for the hydrogen protons. The classification of the hydrogen protons in the

coumarin lactone ring is as follows: H-a at 6.18 ppm (1H, d), H-b at 7.92 ppm (1H, d), H-c at 7.02 ppm (1H, s), and H-d at 6.77 ppm (1H, s). Figure S2(b) depicts the ^{13}C-NMR spectrum of DDCm-EP, with DMSO-d_6 as the selected solvent. The spectrum shows C signal peaks that encompass the carbon atoms of the coumarin group and the carbamate-bonded carbonyl carbon atoms. The signals for the carbon atoms in the coumarin lactone ring range from 102.99 to 149.08 ppm (a-i), while the signals for the carbonyl carbon atoms in the carbamate bond are observed at 156.46 ppm (k) and 143.33 ppm (j). Due to the small amount of DDCm-OH added, the corresponding nuclear magnetic resonance intensity of the carbon atoms is low. The carbon atom classifications are as follows: 161.28 ppm (C-a), 111.67 ppm (C-b), 143.11 ppm (C-c), 110.99 ppm (C-d), 112.54 ppm (C-e), 144.89 ppm (C-f), 147.75 ppm (C-g), 102.99 ppm (C-h), and 149.08 ppm (C-i).

Additionally, DDCm-OH was characterized using ^{1}H-NMR and ^{13}C-NMR, with DMSO-d_6 as the selected solvent. Figure S2(c) depicts the ^{1}H-NMR spectrum of DDCm-OH. The hydrogen protons on the coumarin lactone ring are located in the low-field region, with signals observed at 6.19 ppm (1H, d) attributed to H-a, 7.88 ppm (1H, d) to H-b, 7.03 ppm (1H, s) to H-c, and 6.80 ppm (1H, s) to H-d. Because of the nuclear magnetic instability of the phenol hydroxyl group, the signal at 9.84 ppm (1H, brs) is assigned to H-e. Figure S2(d) displays the ^{13}C-NMR spectrum of DDCm-OH. In this spectrum, the signals are as follows: 161.26 ppm corresponds to C-a, 111.94 ppm to C-b, 143.31 ppm to C-c, 111.22 ppm to C-d, 112.77 ppm to C-e, 144.84 ppm to C-f, 148.95 ppm to C-g, 103.11 ppm to C-h, and 150.82 ppm to C-i. As observed in Figure S2, the peak positions of the hydrogen proton and the carbon atoms in the DDCm-EP coumarin lactone ring are essentially consistent with those in DDCm-OH. Consequently, the results indicate that the ^{1}H-NMR and ^{13}C-NMR peak signals of DDCm-EP are in agreement with the predictions, thereby fully confirming that the structure of DDCm-EP aligns with the expected structure.

S2.4. GPC result of DDCm-EP

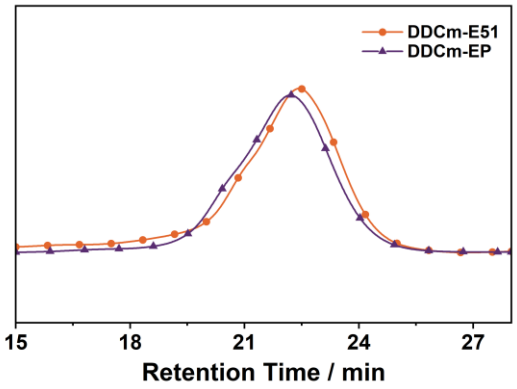

Fig. S3 GPC curves of DDCm-E51 and DDCm-EP in DMF

Table S1 Molecular weights and distributions of DDCm-E51 and DDCm-EP

Samples	Retention time	Mn	Mw	PDI
DDCm-E51	17.25 min	48929 g·mol^{-1}	48985 g·mol^{-1}	1.001
DDCm-EP	16.75 min	53712 g·mol^{-1}	54280 g·mol^{-1}	1.011

DDCm-E51 and DDCm-EP were characterized by gel permeation chromatography. The GPC curves of DDCm-E51 and DDCm-EP were shown in Fig. S3, and the molecular weight data were shown in Table S1. According to the data, it can be observed that the numerical average molecular weight (Mn) of DDCm-EP is 53712 g·mol^{-1}, the weight average molecular weight (Mw) is 54280 g·mol^{-1}, and the dispersion index (PDI) is 1.011. The PDI value of DDCm-EP is close to 1, indicating that the molecular weight distribution of DDCm-EP is relatively concentrated, the polymer chain length is relatively uniform, and the molecular weight polydispersity is not significant. In addition, the molecular weight of DDCm-EP was significantly higher than that of DDCm-E51, which confirmed the successful synthesis of DDCm-EP with higher molecular weight through chemical reaction on the basis of DDCm-E51. In summary, these data indicate that the synthesis process of DDCm-EP is successful, and the resulting products have the expected molecular weight properties.

Supporting information S3

S3.1. Synthesis of MXene/DDCm-EP

Initially, a mixture of 4.2 g IPDI, 1.0 g DDCm-OH, 11.9 g PPG and 7.5 g E51 was introduced into a three-necked flask and stirred at 70℃ under a nitrogen atmosphere for 4 hours to create an epoxy prepolymer incorporating coumarin groups (DDCm-E51). Ultrasonic MXene in THF for 15 minutes to form a uniformly dispersed solution. Subsequently, the MXene solution and 0.9 g curing agent TETA were quickly mixed evenly with DDCm-E51, and then poured into the mold for curing. The mold underwent curing in a blast drying furnace, with the curing process comprising 12 hours at 25℃ and an additional 2 hours at 60℃. After the curing process, the mold was allowed to naturally cool to room temperature, resulting in the formation of a light-triggered self-healing epoxy resin composite film (MXene/DDCm-EP).

Furthermore, the dispersion of MXene in the matrix was observed by SEM, as shown in Fig. S4. It can be seen that 0.5 wt% MXene is uniformly dispersed in the resin matrix. This is due to the interfacial hydrogen bond interaction between MXene and the epoxy matrix, which makes the nanosheets uniformly dispersed in the matrix. In addition, because of the small size and uniform dispersion of MXene, the mechanical properties of the material are significantly improved. This result is consistent with the mechanical properties analysis in section 2.4 of the Manuscript.

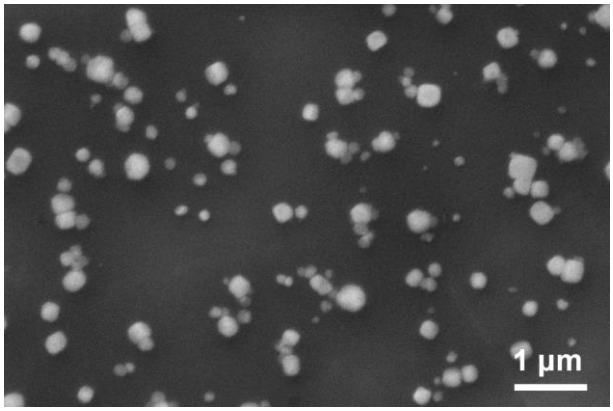

Fig. S4 SEM image of 0.5 wt% MXene/DDCm-EP

S3.2. Thermal properties of MXene/DDCm-EP

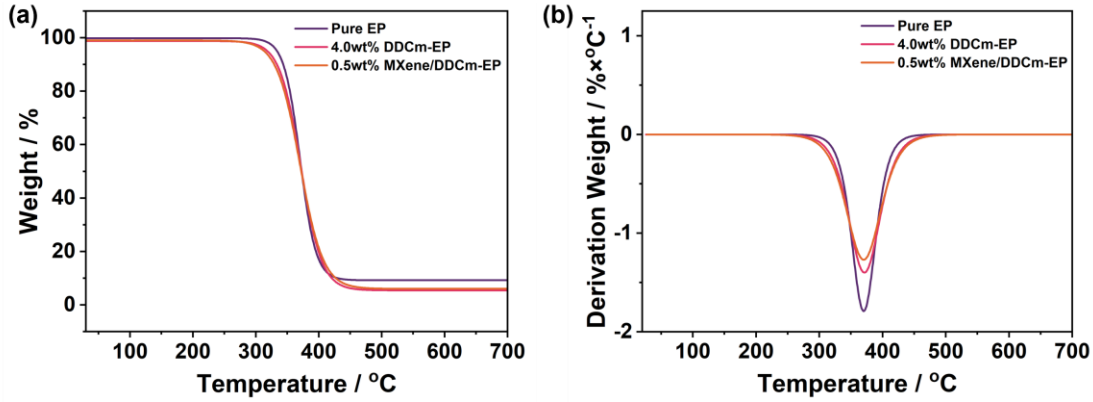

Fig. S5 TGA (a) and DTG (b) curves of 4.0 wt% DDCm-EP and 0.5 wt% MXene/DDCm-EP

The thermal stability of epoxy composite system containing dynamic reversible coumarin groups was tested, and the results were shown in Fig. S5. Thermal degradation behavior and thermal stability can be evaluated by the initial thermal decomposition temperature of the material (the temperature at which the mass loss is 5%, T5%). As can be seen from the figure, both DDCm-EP and MXene/DDCm-EP are one-step thermal degradation processes, indicating that the addition of DDCm-OH and MXene does not change the thermal decomposition mechanism of EP. In addition, the initial thermal decomposition temperature of pure EP is 333.70℃, while the initial thermal decomposition temperature of 4.0 wt% DDCm-EP and 0.5 wt% MXene/DDCm-EP are 306.35℃ and 313.23℃, respectively. The initial thermal decomposition temperature of 4.0 wt% DDCm-EP was reduced by 27.35 ℃ compared to pure EP, a change that can be attributed to the tension energy of the four-membered ring structure in the coumarin dimer with a value of 25.6 kcal·mol^{-1}. This indicates that coumarin groups are less stable than pure EP, and therefore, the addition of coumarin groups to the epoxy resin structure results in a reduction in its thermal stability[1]. Furthermore, when comparing 4.0 wt% DDCm-EP with 0.5 wt% MXene/DDCm-EP, the initial thermal decomposition temperature of the latter increased by 6.88℃. This boost can be attributed to the well-dispersed MXene nanosheets, which allow the material to disperse heat more efficiently and reduce the

formation of hot spots, thereby improving the thermal stability of EP to some extent. Taking the above factors into consideration, although the introduction of coumarin groups led to a decrease in the initial thermal decomposition temperature of epoxy resin, the addition of MXene nanosheets effectively partially offset this adverse effect, making MXene/DDCm-EP composites maintain a high thermal stability on the whole, and its thermal decomposition temperature is similar to the original thermal decomposition temperature of pure EP[2]. This result shows that the composite is able to maintain similar stability to pure epoxy resins at high temperatures, ensuring that its performance in specific applications is not significantly affected.

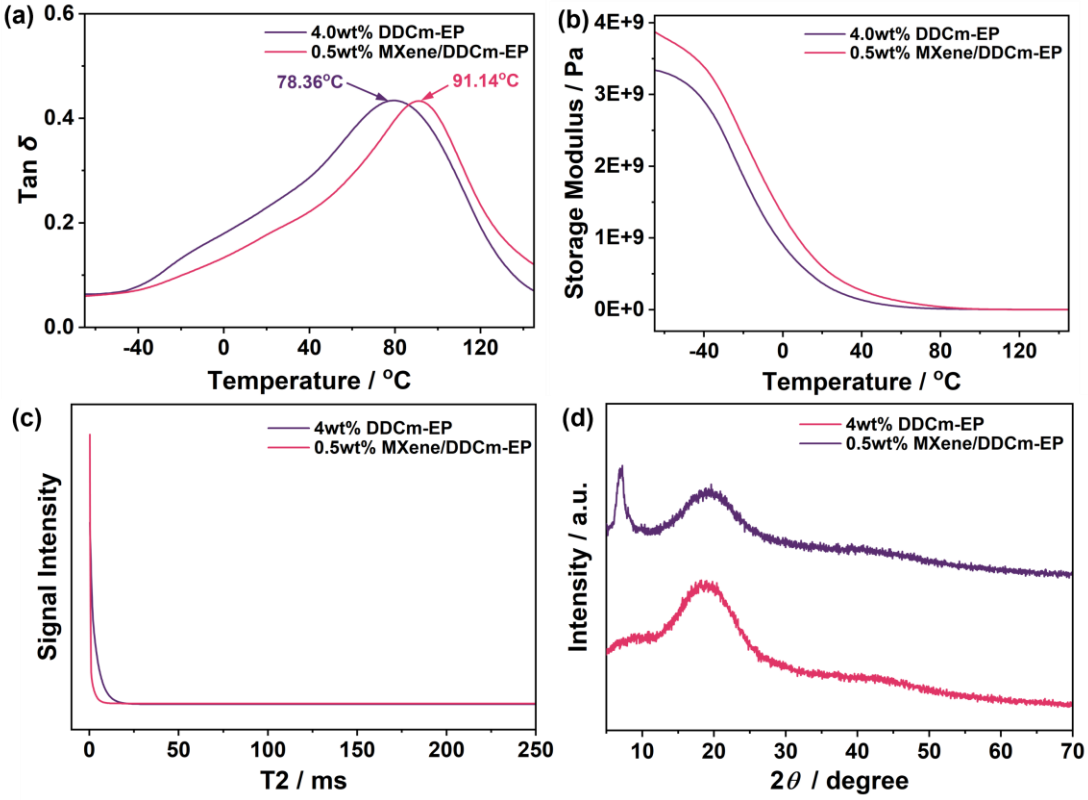

Fig. S6 Tanδ curves (a), storage modulus curves (b), LF-NMR (c), and XRD (d) of 4.0 wt% DDCm-EP and 0.5 wt% MXene/DDCm-EP

The glass transition temperature (Tg) is a key factor affecting the tensile properties of polymers. In order to explore the Tg of 4.0 wt% DDCm-EP and 0.5 wt% MXene/DDCm-EP, DMA was used to test them, and the results were shown in Fig. S6. In Fig. S6(a), the loss factor curve displays a significant feature: throughout the test temperature range, both 4.0 wt% DDCm-EP and 0.5 wt% MXene/DDCm-EP

exhibit clearly single peaks, with no second phase observed. This indicates that MXene nanosheets are compatible well with the DDCm-EP matrix. This compatibility can be attributed to the highly electronegative functional groups -OH and -F on the surface of MXene nanosheets (XPS and element mapping analysis in part 2.3 of the manuscript). These functional groups can interact with hydrogen atoms in the epoxy resin matrix to form hydrogen bonds, enhancing the interfacial binding force between MXene and the epoxy matrix and thus improving the compatibility between the two materials[3-6].

In addition, the temperature corresponding to the peak value of the loss factor curve is the glass transition temperature of the material. Accordingly, Tg of 4.0 wt% DDCm-EP and 0.5 wt% MXene/DDCm-EP can be determined to be 78.36℃ and 91.14℃, respectively. Compared with 4.0 wt% DDCm-EP, Tg of 0.5 wt% MXene/DDCm-EP was increased by 12.78℃. The functional groups -OH and -F on the surface of MXene nanosheets have strong electronegativity. They can interact with hydrogen atoms in the epoxy resin matrix to form hydrogen bonds. This strong hydrogen bond interaction leads to a decrease in the mobility of the molecular chains around the MXene nanosheets, thereby increasing the cross-linking density, which in turn is manifested in an increase in the Tg on the macro level. In addition, this interaction of hydrogen bonds also leads to a decrease in the diffraction intensity of the composite film at 2θ=19°-24° on the XRD pattern[7], as shown in Fig. S6(d). Detailed analysis by LF-NMR shows that, as shown in Fig. S6(c), compared with 4.0 wt% DDCm-EP, the nuclear magnetic resonance signal attenuation of 0.5 wt% MXene/DDCm-EP is faster and the relaxation time is shorter, indicating that the addition of MXene enhances the hydrogen bond interaction between molecular chains of the composite. Resulting in increased crosslinking density, as can be seen from the Table S2. Compared with 4.0 wt% DDCm-EP, 0.5wt% MXene/DDCm-EP formed more hydrogen bonds around the crosslinking point, which means that the hydrogen bond interaction around the crosslinking point was stronger. This action limits the movement of the epoxy chain segments and reduces the free volume, resulting in an

increase in Tg[8-10].

Table S2 LF-NMR data of 4.0 wt% DDCm-EP and 0.5 wt% MXene/DDCm-EP

Samples	Crosslinking density	Mc	A	B	C
4.0 wt% DDCm-EP	1.75E-4 mol·mL^{-1}	6.74 kg·mol^{-1}	28.24%	71.76%	0%
0.5 wt% Mxene/DDCm-EP	3.96 E-4 mol·mL^{-1}	2.98 kg·mol^{-1}	86.31%	13.69%	0%

Note:

The hydrogen proton relaxation time (T2) inside the polymer reflects its chemical environment, which is closely related to the binding force and freedom of the hydrogen proton. The binding degree of hydrogen protons is closely related to the microstructure of the sample network. The relaxation time of hydrogen atom can be divided into three parts: the cross-linked chain part (A), the suspended tail chain part (B) and the free chain part (C). The hydrogen atoms in the cross-linked chain include hydrogen atoms around the cross-linking points and participating in forming hydrogen bonds. The hydrogen atoms in the tail chain part are located in the soft segment far away from the crosslinking point and the tail chain without hydrogen bond formation. The free chain part is mainly composed of small molecules that are not involved in the curing reaction and hydrogen atoms on the free chain[11].

As can be seen from the energy storage modulus curve in Fig. S6(b), the energy storage modulus drops rapidly near the glass transition temperature and then reaches a stable platform modulus, indicating that the cross-linked network maintains stable network connectivity at the test temperature. In addition, it is also observed that the initial energy storage modulus of 0.5 wt% MXene/DDCm-EP increases compared to 4.0 wt% DDCm-EP. This is mainly due to the fact that MXene nanosheets allow stress to be transferred from the epoxy matrix to MXene, thereby improving the stability and load-bearing capacity of the material during its application. It is worth pointing out that because pure EP is difficult to form a uniform film without modification, it directly leads to the failure to test it by DMA under the same experimental conditions. Therefore, this study cannot provide relevant data of loss factor curve and energy storage modulus curve of pure EP.

S3.3. Mechanical properties of MXene/DDCm-EP

Table S3 shows the mechanical properties of DDCm-EP with different DDCm-OH contents, and the specific data of tensile strength, elongation at break and Young's modulus of the resins can be obtained from Table S3. Along with this, Table S4 shows the mechanical properties of MXene/DDCm-EP with different MXene contents, and the specific data of tensile strength, elongation at break and Young's modulus of the composites can be obtained from Table S4.

Table S3 Mechanical properties of DDCm-EP with different DDCm-OH contents

Samples	Stress	Strain	Young's Modulus
Pure EP	1.5 MPa	6.5%	43.2 MPa
3.0 wt% DDCm-EP	3.4 MPa	260.3%	2.5 MPa
4.0 wt% DDCm-EP	3.8 MPa	122.7%	13.6 MPa
5.0 wt% DDCm-EP	1.1 MPa	33.4%	8.5 MPa
6.0 wt% DDCm-EP	1.1 MPa	30.9%	11.6 MPa

Table S4 Mechanical properties of MXene/DDCm-EP with different MXene contents

Samples	Stress	Strain	Young's Modulus
Pure EP	1.5 MPa	6.5%	43.2 MPa
4.0 wt% DDCm-EP	3.8 MPa	122.7%	13.6 MPa
0.25 wt% MXene/DDCm-EP	4.7 MPa	53.5%	20.0 MPa
0.5 wt% MXene/DDCm-EP	16.4 MPa	92.5%	72.2 MPa
1.0 wt% MXene/DDCm-EP	5.5 MPa	101.0%	21.1 MPa
1.5 wt% MXene/DDCm-EP	1.2 MPa	27.8%	10.0 MPa

S3.4. Self-healing performance of MXene/DDCm-EP

In practice manner, Wool and O'Connor proposed a relatively basic method for measuring the healing degree of polymer systems to determine their mechanical properties. This method is commonly used as the fundamental method for measuring the "healing efficiency" of self-healing systems[12,13]. Therefore, the expression of healing efficiency η is shown in formula (1-1):

$$\eta = \frac{K_{healed}}{K_{virgin}} \times 100\% \quad (1\text{-}1)$$

Among them, K_{virgin} represents the tensile strength of the original sample, and K_{healed} represents the tensile strength of the healed sample.

Table S5 shows the mechanical properties of 4.0 wt% DDCm-EP after repair under different conditions, including the tensile strength, elongation at break and Young's modulus of the resin. Table S6 shows the mechanical properties of 0.5 wt% MXene/DDCm-EP under xenon lamp after different repair times, including the tensile strength, elongation at break and Young's modulus of the composite.

Table S5 Mechanical properties of 4.0 wt% DDCm-EP after repair under different conditions

Samples	Stress	Strain	Young's Modulus
4.0 wt% DDCm-EP	3.8 MPa	122.7%	13.6 MPa
UV light for 2 h	1.1 MPa	16.1%	14.8 MPa
UV light for 4 h	1.5 MPa	34.0%	13.8 MPa
UV light for 6 h	2.3 MPa	54.8%	10.7 MPa
Xenon lamp for 2 h	1.4 MPa	31.8%	7.4 MPa
Xenon lamp for 4 h	2.1 MPa	51.5%	8.3 MPa
Xenon lamp for 6 h	3.0 MPa	27.8%	29.3 MPa

Table S6 Mechanical properties of 0.5 wt% MXene/DDCm-EP after different repair time under xenon lamp

Samples	Stress	Strain	Young's Modulus
0.5 wt% MXene/DDCm-EP	16.4 MPa	92.5%	72.2 MPa
Xenon lamp for 2 h	7.5 MPa	26.4%	63.5 MPa
Xenon lamp for 4 h	12.1 MPa	46.6%	62.7 MPa
Xenon lamp for 6 h	16.3 MPa	66.8%	82.9 MPa

In order to reflect the long-term performance of the material in practical use, we conducted multiple self-healing cycles for 0.5 wt% MXene/DDCm-EP, and all repairs were conducted under xenon lamp for 6 h. The tensile strength, elongation at break

and Young's modulus of the composite after multiple repair are shown in Table S7.

Table S7 Mechanical properties of 0.5 wt% MXene/DDCm-EP after multiple repair (under xenon lamp repair for 6 h)

Samples	Stress	Strain	Young's Modulus
0.5 wt% MXene/DDCm-EP	16.4 MPa	92.5%	72.2 MPa
Self repair for the first time	16.3 MPa	66.8%	82.9 MPa
Self repair for the second time	10.1 MPa	40.3%	80.2 MPa
Self repair for the third time	6.9 MPa	18.4%	50.3 MPa

References

[1] Y. Wang, Q. Liu, J. Li, L. Ling, G. Zhang, R. Sun and C. P. Wong, *Polymer*, 2019, **172**, 187-195.

[2] H. Li, L. Wang, S. Xu, H. Li, Y. Dai and A. Zhou, *Polym. Adv. Technol.*, 2023, **34**(2), 769-778.

[3] W. Yang, W. Zhou, N. Ding, S. Shen, D. Gao, D. Puglia, Y. Duan, P. Xu, T. Liu, Z. Wang and P. Ma, *Chem. Eng. J.*, 2024, **497**, 154591.

[4] D. Wang, H. Wei, Y. Lin, P. Jiang, H. Bao and X. Huang, *Compos. Sci. Technol.*, 2021, **213**, 108953.

[5] X. Cao, M. Wu, A. Zhou, Y. Wang, X. He and L. Wang, *e-Polymers*, 2017, **17**(5), 373-381.

[6] R. Cai, J. Zhao, N. Lv, A. Fu, C. Yin, C. Song and M. Chao, *Nanomaterials*, 2022, **12**(13), 2249.

[7] Y. Liu, J. Zhang, X. Zhang, Y. Li and J. Wang, *ACS Appl. Mater.*, 2016, **8**(31), 20352-20363.

[8] R. P. White and J. E. Lipson, *Macromolecules*, 2016, **49**(11), 3987-4007.

[9] M. Song, X. L. Yue, X. J. Wang, F. Y. Cao, Y. N. Li, C. H. Su and Q. Qin, *Macromol. Mater. Eng.*, 2020, **305**(8), 2000222.

[10] T. Zhou, C. Zhao, Y. Liu, J. Huang, H. Zhou, Z. Nie, M. Fan, T. Zhao, Q. Cheng and M. Liu, *ACS Nano*, 2022, **16**(8), 12013-12023.

[11] Y. Zhou, L. Zhu, J. Zhai, R. Yang and X. Guo, *Polymer*, 2023, **285**, 126356.

[12] R. P. Wool and K. M. O'Connor, *Appl. Phys. Lett.*, 1981, **52**, 5953-5963.

[13] E. N. Brown, N. R. Sottos and S. R. White, *Exp. Mech.*, 2002, **42**, 372-379.